Journal of Power Sources 219 (2012) 106–111

Contents lists available at SciVerse ScienceDirect

Journal of Power Sources

journal homepage: www.elsevier.com/locate/jpowsour

Short communication

Tungsten carbide promoted Pd and Pd–Co electrocatalysts for formic acid electrooxidation

Min Yin [a,b], Qingfeng Li [a,*], Jens Oluf Jensen [a], Yunjie Huang [a], Lars N. Cleemann [a], Niels J. Bjerrum [a], Wei Xing [b,**]

[a] Department of Energy Conversion and Storage, Kemitorvet 207, Technical University of Denmark, DK-2800 Lyngby, Denmark
[b] Laboratory of Advanced Power Sources, Changchun Institute of Applied Chemistry, Chinese Academy of Sciences, Changchun 130022, PR China

HIGHLIGHTS

- Carbon support functionalized by facilely obtained tungsten carbide.
- Palladium-based nanoparticles supported on the functionalized carbon synthesized.
- Superior activity and stability achieved with the PdCo/WC-C catalyst.
- Synergetic effects among Pd, Co ad WC proposed for the catalytic process.

ARTICLE INFO

Article history:
Received 22 April 2012
Received in revised form
29 June 2012
Accepted 13 July 2012
Available online 20 July 2012

Keywords:
Catalysts
Electrooxidation
Formic acid
Palladium-cobalt
Tungsten carbide

ABSTRACT

Tungsten carbide (WC) promoted palladium (Pd) and palladium–cobalt (Pd–Co) nanocatalysts are prepared and characterized for formic acid electrooxidation. The WC as the dopant to carbon supports is found to enhance the CO tolerance and promote the activity of the Pd-based catalysts for formic acid oxidation. Alloying of Pd with Co further improves the electrocatalytic activity and stability of the WC supported catalysts, attributable to a synergistic effect of the carbide support and PdCo alloy nanoparticles.

1. Introduction

As a potential fuel, the formic acid electro oxidation (FAEO) has attracted recent attention because of its easy storage, low crossover rate through electrolyte membranes and therefore high feeding concentrations compared to methanol as well as fast electrode kinetics [1–3]. Pt and Pd are the most widely employed catalyst for the FAEO. It was suggested that FAEO proceeds via a dual mechanism, a direct and an indirect pathway, the latter being involved in formation of the strongly poisoning CO [4]. On Pd-based catalysts, the FAEO primarily occurs through the direct path and therefore exhibit higher catalytic performance than that on Pt. However, the high performance of Pd catalysts is not sustained for extended time periods [5]. Thus, to improve the activity as well as the stability of Pd catalysts, much effort has been focused on binary metallic catalysts such as PdCo [6,7], PdPt [8], PdIr [9] and PdSn [10,11].

Recent attempts were made to use structured carbon supports such as carbon nanotubes [12] and mesoporous carbon [13]. Of more interest would be introduction of support materials with co-catalytic functionalities with metal nanoparticles as an approach to improve both activity and stability of the catalyst. Tungsten-based materials have recently been studied as novel supports due to their chemical and electrochemical activities and stabilities for various reactions [14,15]. For instance, tungsten carbide was suggested to be able to facilitate the methanol electrooxidation on Pt catalysts [16–18]. PdNi alloys supported on tungsten carbide (WC) were reported to be a Pt-free catalyst for the hydrogen oxidation reaction [19]. Chhina et al. found out that WC could help retain the surface area and activity of Pt during a corrosion test in acid due to a passive WO_x shell encapsulating the carbide core [19]. In the

* Corresponding author. Tel.: +45 4525 2318.
** Corresponding author. Tel.: +86 43185262223.
E-mail addresses: qfli@dtu.dk (Q. Li), xingwei@ciac.jl.cn (W. Xing).

0378-7753/$ – see front matter © 2012 Elsevier B.V. All rights reserved.
http://dx.doi.org/10.1016/j.jpowsour.2012.07.032

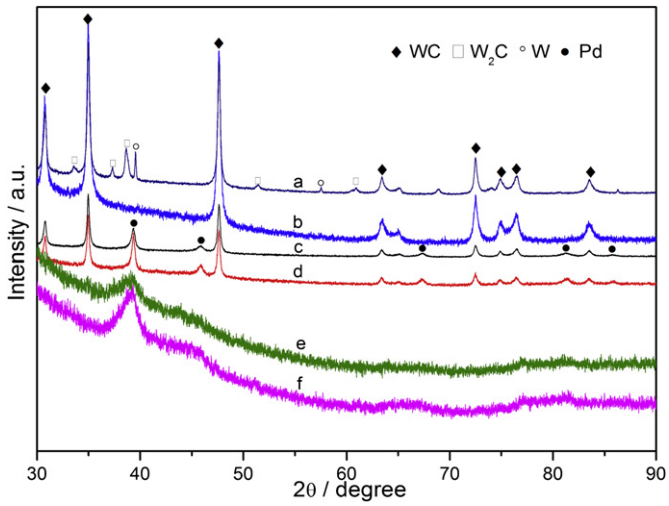

Fig. 1. XRD for WC-C a) before and b) after NaOH treatment, c) Pd/C, d) PdCo/C, e) Pd/WC-C, and f) PdCo/WC-C samples.

present study, tungsten carbide doped carbon supports were prepared, based on which Pd and PdCo catalysts were synthesized and evaluated for direct oxidation of formic acid.

2. Experimental section

2.1. Preparation of tungsten carbide modified carbon supports

WC was coated on Vulcan XC-72R carbon black by carbothermal synthesis. The carbon black was first ultrasonically suspended in water, into which an aqueous ammonium metatungstate (AMT) solution was added. The AMT impregnated carbon was then dried at 100 °C under vacuum, followed by a heat treatment at 900 °C in N_2. Thus obtained WC modified carbon black was further treated in 1 M NaOH for 24 h before use in order to remove the W_2C and impurities, as to be discussed later.

2.2. Preparation of electrocatalysts

The PdCo/C electrocatalysts were typically synthesized as follows. 240 mg of the support was first dispersed in 250 mL deionized water containing 4 g β-D-glucose. 50 mL of a mixture solution containing 0.50 mmol $(NH_4)_2PdCl_4$ and 0.125 mmol $CoCl_2 \cdot 6H_2O$ (4:1 molar ratio of Pd:Co) was slowly added into the suspension. The pH of this suspension was then tuned to 10 by adding 0.1 M NaOH. An aqueous $NaBH_4$ solution in a tenfold excess was used as the reducing agent at room temperature. The catalyst was finally filtered, washed and finally dried at 70 °C. The same procedure was used to synthesize Pd/C, Pd/WC-C, and PdCo/WC-C catalyst by using the appropriate precursors and supports. The metal (Pd or PdCo) catalyst loading of all these catalysts was 20 wt%.

2.3. Material characterizations

The crystal structure of the prepared samples was verified by X-ray diffraction (XRD) using a Huber G670 X-ray diffractometer with a copper rotating anode (CuK radiation, $\lambda = 1.54056$ Å). Transmission electron microscopy (TEM) and high resolution TEM (HRTEM) analysis were carried out with a JEOL2100F microscope operating at 200 kV. Samples were first ultrasonicated in alcohol for 1 h and then deposited on 3 mm Cu grids. X-ray photoelectron spectroscopy (XPS) was performed on a Kratos XSAM-800 spectrometer with an Al Kα monochromatic source. Electrochemical

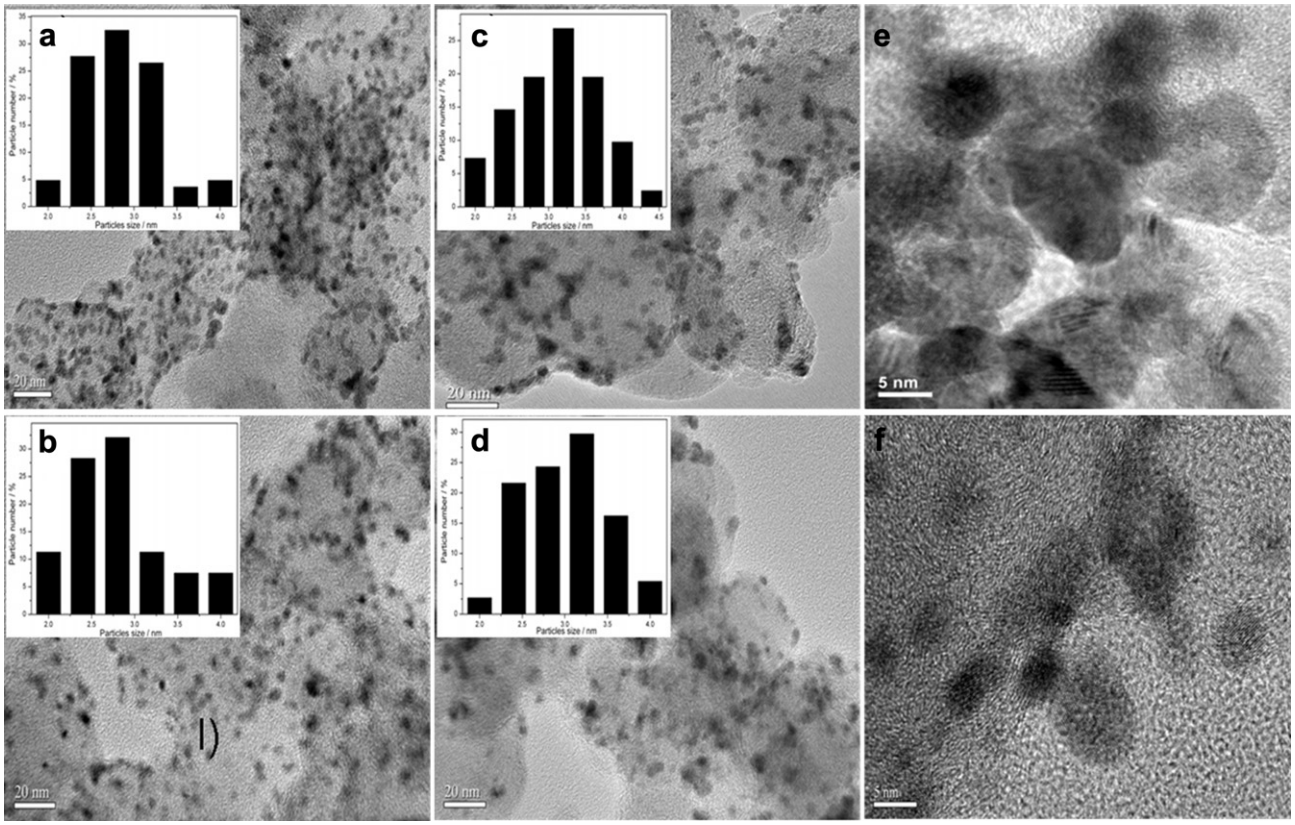

Fig. 2. TEM images of a) Pd/C, b) PdCo/C, c) Pd/WC-C, and d) PdCo/WC-C and HRTEM images of e) WC-C and f) PdCo/WC-C. The insets in a), b), c), and d) are the corresponding particle size distribution histograms of each sample.

measurements were carried out at room temperature with a Princeton Versastat 3 Potentiostat with a Pt coil as the counter electrode and a saturated calomel electrode (SCE) as the reference electrode. For the working electrode, 5 mg of a catalyst was dispersed ultrasonically in 1 ml of ethanol containing 50 μl of 5% Nafion. 4.2 μL of the dispersion was pipetted onto a polished glassy carbon electrode. Cyclic voltammograms (CVs) were recorded in the 0.5 M H_2SO_4 electrolyte containing 0.5 M HCOOH. Chronoamperometric (CA) measurements were made under a constant potential of 0.445 V vs RHE. For CO stripping tests, the CO adsorption onto the catalyst was achieved at a constant potential of 0.1 V in the 0.5 M H_2SO_4 solution during the bubbling of a mixture of 5% CO in hydrogen for 30 min. The excess CO in the electrolyte was then removed by bubbling N_2 for 30 min, after which the stripping voltammograms were recorded as a scan rate of 20 mV s^{-1}.

3. Results and discussions

Fig. 1 shows the XRD patterns of the samples. For the WC-C sample before the NaOH treatment, the main diffraction peaks at 30.77°, 34.96°, and 47.72° were observed, corresponding to the (001), (100), and (101) planes of WC with a hexagonal closed-packed structure. The weak diffraction peaks at 33.6, 37.4, and 38.7° were assigned to the (002), (200), (102) planes of W_2C and the peak at 39.6° to the (110) plane of the tungsten metal. It has been reported that W_2C is instable in either alkaline or acidic media and its oxidation starts at potentials of as low as 0.2 V versus RHE [20]. The pure phase of WC is hence desirable for fuel cell applications. In this work, the obtained samples were treated in 1 M NaOH solution in order to remove the W_2C and W impurities in the as-prepared samples. It can be clearly seen from XRD results that the W_2C and W phases were completely removed after the post-treatment while the WC phase remained. The XRD patterns for Pd in the as-prepared catalysts exhibited five characteristic peaks of the face-centered cubic (fcc) structure, corresponding to the planes (111), (200), (220), (311) and (222) of Pd. A slight shift in the diffraction peaks for PdCo electrocatalysts was observed towards higher 2θ as compared with the corresponding ones for pure Pd, showing a Pd lattice contraction due to PdCo alloying, as reported previously [7,12,21].

Fig. 2 displays the TEM images and the corresponding size distribution histograms of each catalyst. The Pd and PdCo nanoparticles were dispersed uniformly on both carbon and WC modified carbon supports and had a rather narrow size distribution with an average particle size from 2.8 to 3.0 nm for all four types of catalysts, i.e. Pd/C, PdCo/C, Pd/WC-C and PdCo/WC-C. The HRTEM image of WC-C in Fig. 2e showed the modified WC at the surface of carbon with a diameter range from 6 to 10 nm. As observed from the HRTEM image of PdCo/WC-C in Fig. 2f, the metal nanoparticles and WC particles in a spherical shape overlay mutually at the surface of carbon.

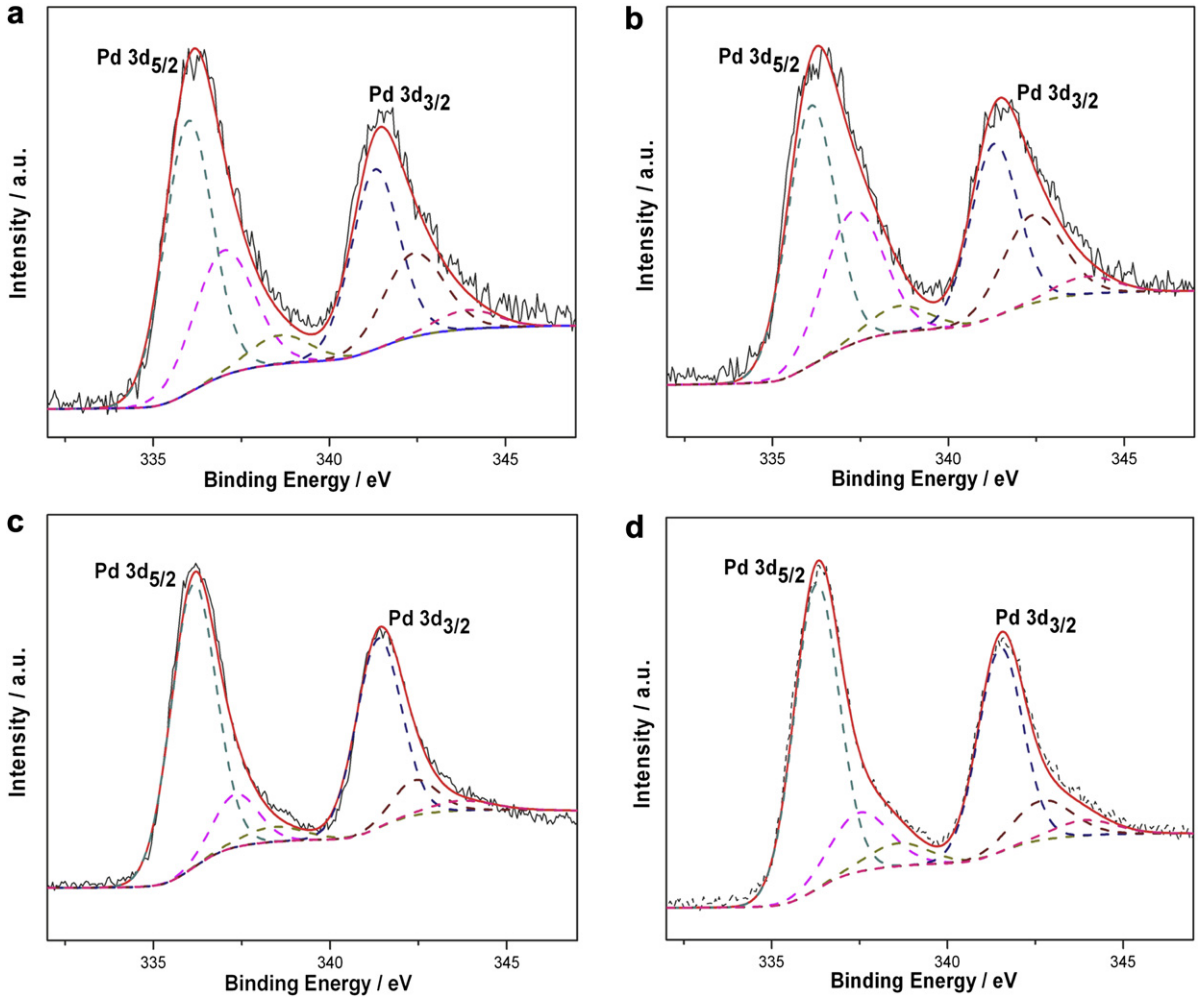

Fig. 3. XPS spectra of a) Pd/C, b) PdCo/C, c) Pd/WC-C, and d) PdCo/WC-C.

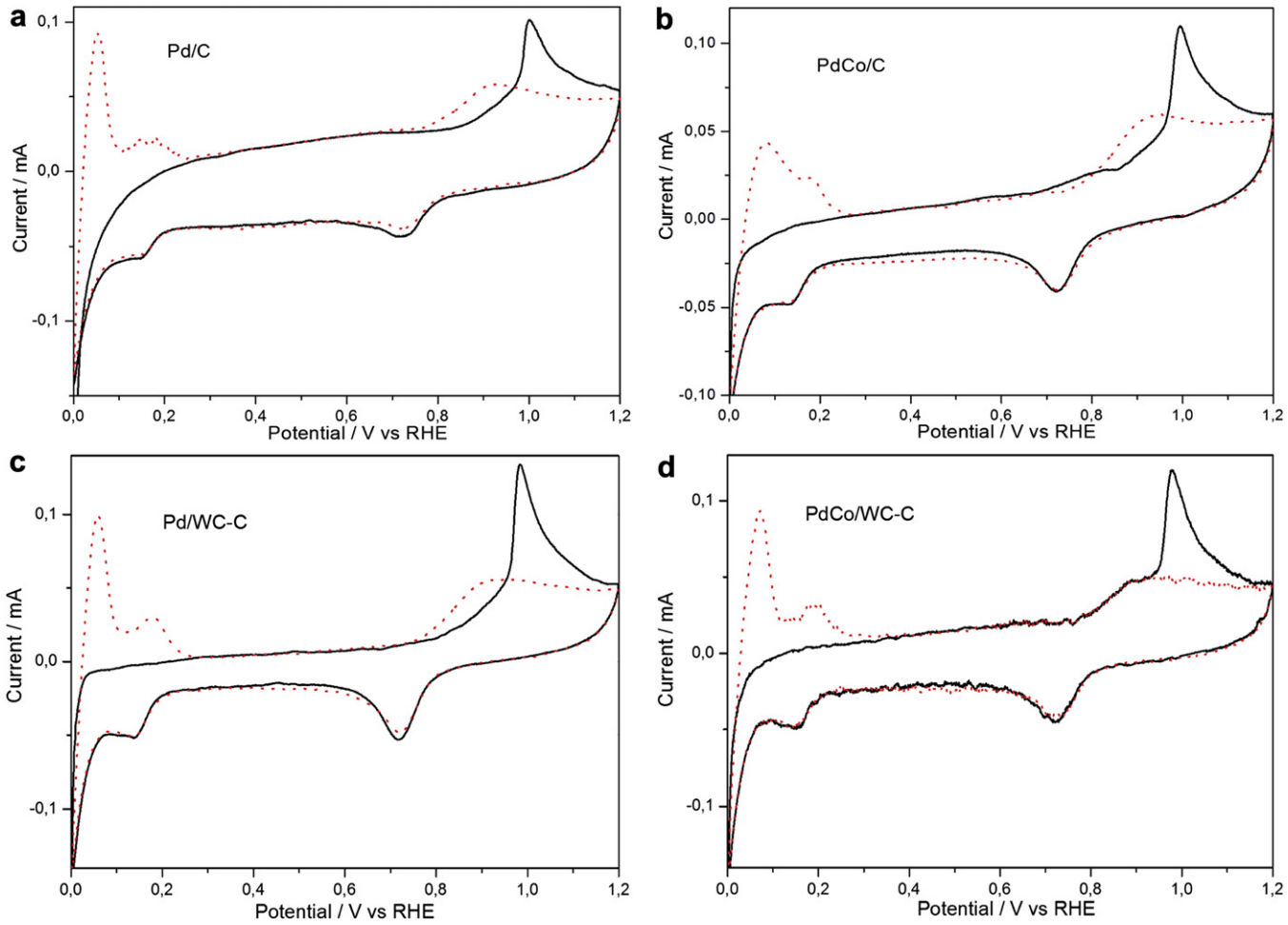

Fig. 4. CO-stripping voltammograms on a) Pd/C, b) PdCo/C, c) Pd/WC-C, and d) PdCo/WC-C electrodes in 0.5 M H_2SO_4 solutions at a scan rate of 20 mV s^{-1} with the first cycle (black solid line) and the second cycle (red dashed line). (For interpretation of the references to color in this figure legend, the reader is referred to the web version of this article.)

XPS was then used to determine the possible electronic interactions between the support and the metal particles. As shown in Fig. 3, the Pd 3d signals of each sample were deconvolved into three components assigned to metallic Pd, Pd (II) and Pd (IV) species. The $3d_{5/2}$ binding energies of Pd species showed a shift from 336.0 for Pd/C to 336.1 for PdCo/C, 336.13 for Pd/WC-C and 336.27 eV for PdCo/WC-C as a result of modification by Co and WC. As Shen et al. [22] has reported the modified electronic properties of Pt by WC on Pt/WC-C catalysts, the metal-support interactions between Pd and WC could likely be the explanation for these observations [23].

To evaluate the resistance to the CO_{ads} poisoning of each catalyst, the CO-stripping voltammograms were recorded, as shown in Fig. 4. The electrochemical surface area (ECSA) of each catalyst was calculated by the following equation, where Q_{CO} is the columbic charge for the CO_{ads} oxidation, m is the metal mass on the electrode, 420 μC cm^{-2} is the assumed columbic charge required for the oxidation of a CO_{ads} monolayer [24].

$$\mathrm{ECSA}\left(\mathrm{m^2\ g^{-1}}\right) = \frac{Q_{CO}(\mu C)}{420(\mu C\ cm^{-2})}\ \frac{100}{m(\mu g)}$$

The calculated ECSA values are listed in Table 1. As also listed in the table, a negative shift of the well-defined CO stripping current peak was observed from 1002 mV for the Pd/C to 975 mV for the PdCo/WC-C catalyst, indicating the effect of Co and WC in the catalysts on weakening the CO adsorptive bond on the Pd active sites.

The formic acid electrooxidation on these catalysts was investigated by cyclic voltammetry, as shown in Fig. 5a. A typical current peak associated to the FAEO was observed on the Pd-based catalysts. It was slightly shifted in the negative direction for the PdCo/C and Pd/WC-C catalysts, as compared with the Pd/C catalyst. The onset potential of the FAEO for PdCo/WC-C was also found to be shifted negatively by ca. 20 mV compared with that for the Pd/C catalyst. This indicated the favorable effect of Co and WC in the catalysts on the FAEO, most likely due to cooperative synergies of Co and WC. Furthermore, the specific currents for the FAEO of the four catalysts at 0.3 V are listed in Table 1. Addition of Co into the Pd electrocatalyst led to a 1.25-folder increase in the formic acid electrooxidation current, which is in good agreement with the results reported by others [7,12]. It is interesting that using the WC

Table 1
ECSA and catalytic activities towards FAEO of different catalysts.

	Pd/C	PdCo/C	Pd/WC-C	PdCo/WC-C
ECSA ($m^2\ g^{-1}$)	52.4	66.1	55.9	58.9
Peak potential for CO oxidation (mV vs. RHE)	1002	992	983	975
Specific current for FAEO ($mA\ cm^{-2}$) at 0.3 V	0.4	0.9	1.2	1.7
Tafel slope for FAEO ($mV\ dec^{-1}$)	188	158	114	73
Stable current density after 3600 s in CA at 0.445V vs RHE ($mA\ cm^{-2}$)	0.012	0.034	0.14	0.21

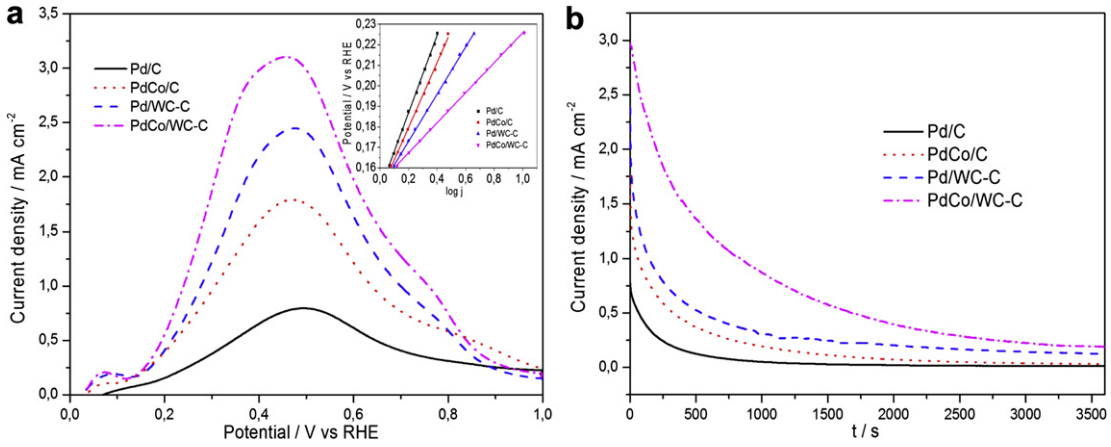

Fig. 5. a) CVs of each catalyst in N_2-satruated 0.5 M HCOOH + 0.5 M H_2SO_4 solutions at a scan rate of 50 mV s^{-1}. The current density is based on the electrochemical surface area. Inset: Tafel plots of each catalyst at a scan rate of 1 mV s^{-1}. The current (j) is normalized to the geometric electrode area. b) Amperometric i–t curves of HCOOH electro-oxidation on each catalyst in N_2-saturated 0.5 M HCOOH + 0.5 M H_2SO_4 at a fixed potential of 0.445 V vs RHE. The current density is based on the electrochemical surface area.

doped carbon support further improved the catalytic activity for both Pd and PdCo catalysts towards the formic acid oxidation. The best catalytic activity for the FAEO was observed on the PdCo/WC-C catalyst, which was 3 times higher than that of the Pd/C catalyst on the basis of the specific surface area of the catalysts.

These results may be attributed to the following reasons. First of all, the XPS results showed the positive shift in binding energies for Co and WC doped Pd catalysts, indicating the changed electronic structure and density of the state of Pd nanoparticles due to the strong intermetallic binding among Pd, Co and WC. Previous reports have shown that the Pd nanoparticles with higher BE displayed an increased catalytic activity for the FAEO [25], which was attributed to a decreased adsorption energy of the formic intermediates and intrinsically enhanced catalytic rate of the FAEO. The higher BE indicated from the above XPS results in this study for the WC and Co doped Pd nanoparticles suggested an accelerated kinetic rate of the FAEO. Secondly, the CO-like species on the Pd surface during the FAEO could be oxidatively removed by a similar bifunctional mechanism, in which the oxygen-containing species existed on a neighboring surface site and facilitated the CO-like species removed [26]. Here, formation of the hydrogen tungsten bronze in an electrochemical environment [27,28] could promote the dissociation of H_2O into H^+ and OH^-, provide more OH_{ad} species to the catalytic sites and accelerate the CO oxidation and removal. The inset of Fig. 5a shows the Tafel plots for the FAEO on these catalysts. The values of Tafel slopes were found to decrease in the order of Pd/C > PdCo/C > Pd/WC-C > PdCo/WC-C, which indicated that the rate of the charge-transfer kinetics of the formic acid electroxidation was truly increased by introducing Co, WC and their combination in the catalysts.

Fig. 5b shows the chronoamperometric curves for the four types of catalysts at 0.445 V vs RHE in the 0.5 M H_2SO_4 + 0.5 M HCOOH solution. The oxidation current densities on Pd/C and PdCo/C electrodes decreased exponentially with time at the beginning and reached a more or less constant value after hundreds of seconds. Only 2% of the initial activity was retained after 3600 s of the chronoamperometry on the Pd/C catalyst, while 3.3% of the initial activity could be maintained on the PdCo/C catalyst, confirming the slightly better electrocatalytic stability of the PdCo alloy catalyst. This is coincided with the recent results [12], where the electrocatalytic stability was concluded for the Pd–Co catalysts supported on multi-walled carbon nanotubes. A slower current decay was observed on the WC supported catalysts, compared with that on the carbon supported catalysts, with 6.6% of the retained activity on the Pd/WC-C and 7.8% on the PdCo/WC-C catalyst after 3600 s. The final constant currents on the Pd/WC-C and PdCo/WC-C catalysts were found to be 0.14 and 0.22 mA cm^{-2}, respectively, also significantly superior to the PdCo/C (0.012 mA cm^{-2}) and Pd/C (0.034 mA cm^{-2}) catalysts. This result revealed the synergistic interactions of WC and Pd-based catalysts, leading to both promotion and stabilization of the catalytic activity for the FAEO.

4. Conclusions

Tungsten carbide as the catalyst support was found to weaken the CO bonding and enhance the catalytic activity towards the formic acid oxidation on the Pd-based catalysts. The alloying of Pd with Co and doping of carbon supports with tungsten carbide, i.e. in form of the PdCo/WC-C catalyst, showed substantial promotion of the catalytic activity and superior stability for the formic acid oxidation. Both effects were attributed to the synergistic effects of WC and Pd–Co nanoparticles.

Acknowledgements

This work was jointly supported by the Danish National Research Foundation and Nature Science Foundation of China (project no. 21011130027) through the Danish-Chinese Centre for Proton Conducting Systems. National Natural Science Foundation of China (21073180, 20933004), 973 Program (2012CB215500) and 863 program (SS2012AA053401) are also acknowledged.

References

[1] J.L. Haan, K.M. Stafford, R.D. Morgan, R.I. Masel, Electrochim. Acta 55 (2010) 2477.
[2] S. Ha, R.I. Masel, J. Power Sources 144 (2005) 28.
[3] J.Y. Wang, H.X. Zhang, K. Jiang, W.B. Cai, J. Am. Chem. Soc. 133 (2011) 14876.
[4] S. Park, Y. Xie, M.J. Weaver, Langmuir 18 (2002) 5792.
[5] X.W. Yu, P.G. Pickup, Electrochem. Commun. 11 (2009) 2012.
[6] C. Jung, C.M. Sanchez-Sanchez, C.-L. Lin, J. Rodriguez-Lopez, A.J. Bard, Anal. Chem. 81 (2009) 7003.
[7] X. Wang, Y. Xia, Electrochem. Commun. 10 (2008) 1644.
[8] E.A. Baranova, N. Miles, P.H.J. Mercier, Y. Le Page, B. Patarachao, Electrochim. Acta 55 (2010) 8182.
[9] X. Wang, Y. Tang, Y. Gao, T. Lu, J. Power Sources 175 (2008) 784.
[10] Z. Liu, X. Zhang, Electrochem. Commun. 11 (2009) 1667.
[11] Z. Zhang, J. Ge, L. Ma, J. Liao, T. Lu, W. Xing, Fuel Cells 9 (2009) 114.
[12] D. Morales-Acosta, J. Ledesma-Garcia, L.A. Godinez, H.G. Rodriguez, L. Alvarez-Contreras, L.G. Arriaga, J. Power Sources 195 (2010) 461.
[13] T. Maiyalagan, A.B.A. Nassr, T.O. Alaje, M. Bron, K. Scott, J. Power Sources 211 (2012) 147.
[14] J.B. Christian, S.P.E. Smith, M.S. .Whittingham, H.D. Abruna, Electrochem. Commun. 9 (2007) 2128.

[15] C. Liang, L. Ding, C. Li, M. Pang, D. Su, W. Li, Y. Wang, Energy Environ. Sci. 3 (2010) 1121.
[16] R. .Wang, C. Tian, L. Wang, B. Wang, H. Zhang, H. Fu, Chem. Commun. 21 (2009) 3104.
[17] M.K. Jeon, H. Daimon, K.R. Lee, A. Nakahara, S.I. Woo, Electrochem. Commun. 9 (2007) 2692.
[18] P.K. Shen, S. Yin, Z. Li, C. Chen, Electrochim. Acta 55 (2010) 7969.
[19] D.J. Ham, C. Pak, G.H. Bae, S. Han, K. Kwon, S.A. Jin, H. Chang, S.H. Choi, J.S. Lee, Chem. Commun. 47 (2011) 5792.
[20] M.B. Zellner, J.G.G. Chen, Cataly. Today 99 (2005) 299.
[21] Y.C. Wei, C.W. Liu, Y.W. Chang, C.M. Lai, P.Y. Lim, L.D. Tsai, K.W. Wang, Int. J. Hydrogen Energy 35 (2010) 1864.
[22] G. Cui, P.K. Shen, H. Meng, J. Zhao, G. Wu, J. Power Sources 196 (2011) 6125.
[23] L. Ma, X. Zhao, F.Z. Si, C.P. Liu, J.H. Liao, L. Liang, W. Xing, Electrochim. Acta 55 (2010) 9105.
[24] X. .Zhao, J.B. Zhu, L. Liang, C.P. Liu, J.H. Liao, W. Xing, J. Power Sources 210 (2012) 392.
[25] W.P. Zhou, A. Lewera, R. Larsen, R.I. Masel, P.S. Bagus, A. Wieckowski, J. Phys. Chem. B 110 (2006) 13393.
[26] X. Zhao, M. Yin, L. Ma, L. Liang, C.P. Liu, W. Xing, Energy Environ. Sci. 4 (2011) 2736–2753.
[27] P.K. Shen, A.C.C. Tseung, J. Electrochem. Soc. 141 (1994) 3082.
[28] S. Yin, M. Cai, C. Wang, P.K. Shen, Energy Environ. Sci. 4 (2011) 558.